

Polarization singularities and Möbius strips in sound and water-surface waves

Konstantin Y. Bliokh,¹ Miguel A. Alonso,^{2,3} Danica Sugic,¹ Mathias Perrin,⁴ Franco Nori,^{1,5,6} and Etienne Brasselet⁴

¹Theoretical Quantum Physics Laboratory, RIKEN Cluster for Pioneering Research, Wako-shi, Saitama 351-0198, Japan

²CNRS, Centrale Marseille, Institut Fresnel, Aix Marseille University, UMR 7249, 13397 Marseille CEDEX 20, France

³The Institute of Optics, University of Rochester, Rochester, NY 14627, USA

⁴Université de Bordeaux, CNRS, LOMA, UMR 5798, Talence, France

⁵RIKEN Center for Quantum Computing, Wako-shi, Saitama 351-0198, Japan

⁶Physics Department, University of Michigan, Ann Arbor, Michigan 48109-1040, USA

We show that polarization singularities, generic for any complex vector field but so far mostly studied for electromagnetic fields, appear naturally in inhomogeneous yet monochromatic sound and water-surface (e.g., gravity or capillary) wave fields in fluids or gases. The vector properties of these waves are described by the velocity or displacement fields characterizing the local oscillatory motion of the medium particles. We consider a number of examples revealing C-points of purely circular polarization and polarization Möbius strips (formed by major axes of polarization ellipses) around the C-points in sound and gravity wave fields. Our results (i) offer a new readily accessible platform for studies of polarization singularities and topological features of complex vector wavefields and (ii) can play an important role in characterizing vector (e.g., dipole) wave-matter interactions in acoustics and fluid mechanics.

I. INTRODUCTION

Polarization and spin are inherent properties of vector waves. These are typically associated with classical electromagnetic/optical fields or quantum particles with spin [1–3]. Recently, it was noticed that sound waves in fluids or gases [4–10] as well as water-surface (e.g., gravity) waves [11, 12] also possess inherent vector properties, and the notions of polarization and spin are naturally involved there (see also earlier Refs. [13, 14]). These properties are related to the wave-induced motion of the medium’s particles. Such motion can be characterized by the vector velocity field $\mathbf{V}(\mathbf{r}, t)$ or the corresponding displacement field $\mathcal{R}(\mathbf{r}, t)$, $\mathbf{V} = \partial_t \mathcal{R}$, in a way entirely analogous to, e.g., the electric field $\mathcal{E}(\mathbf{r}, t)$ or the corresponding vector-potential $\mathcal{A}(\mathbf{r}, t)$, $\mathcal{E} = -\partial_t \mathcal{A}$, in an electromagnetic wave.

The main difference between electromagnetic and sound-wave polarizations is that the former are *transverse* (the fields \mathcal{E} and \mathcal{A} are orthogonal to the wavevector \mathbf{k} for a plane wave), while the latter are *longitudinal* (the fields \mathbf{V} and \mathcal{R} are parallel to the wavevector for a plane wave). In the case of gravity or capillary waves, which appear on surfaces of classical fluids or gases [15], a plane wave has a *mixed* nature. Namely, the fields \mathbf{V} and \mathcal{R} have longitudinal components along the wavevector lying in the unperturbed water-surface plane, as well as vertical components normal to the surface and the wavevector. Akin to other surface or evanescent waves [4, 5, 16, 17], these two components are mutually $\pi/2$ phase-shifted, so that gravity plane waves are *elliptically* polarized in the propagation plane [18].

However, when one considers structured (inhomogeneous) wave fields, consisting of many plane waves, these differences between transverse, longitudinal, and mixed plane-wave polarizations are largely eliminated. Indeed, at a given point \mathbf{r} , a vector monochromatic field, whether electromagnetic, acoustic, or water-surface, traces an el-

lipse which can have arbitrary orientation in 3D. Considering the spatial distribution of such ellipses across the \mathbf{r} -space, one deals with inhomogeneous polarization textures. Important generic and topologically-robust characteristics of inhomogeneous wave fields are *singularities*: phase singularities in scalar fields and *polarization singularities* in vector polarization fields [19].

In physics of fluids, the emergence of various singularities is a longstanding problem attracting continuous interest [20, 21]. In particular, the topological nature of singularities allows one to use these for the characterization of complex flows (e.g., vortices in turbulence). Furthermore, singularities can be closely related to the formation of robust topologically nontrivial objects, such as knots [22, 23] or Möbius strips [24, 25].

Therefore, it is not surprising that both phase singularities and 2D polarization singularities in wave fields were first observed in the scalar and 2D-current representations of tidal ocean waves [26–29]. However, a systematic treatment of structured wave fields has only been developed within the framework of *singular optics* [19, 30–32]. According to this approach, generic singularities of 2D (paraxial) and 3D (nonparaxial) polarization fields are *C-points* or C-lines of purely circular polarizations as well as *L-lines* or L-surfaces of purely linear polarizations [19, 30, 32–35], and *polarization Möbius strips* [35–44] which are formed (solely in 3D fields) by major axes of polarization ellipses around C-points/lines. These objects are very robust because of their topological nature; they also have important implications in the geometric-phase and angular-momentum properties of the field [35].

Being thoroughly described and observed for optical fields, polarization singularities and topological polarization structures have not been examined properly in sound and water waves. In this work, we fill this gap. We consider both random and regular structured acoustic and water-surface wavefields and show that polarization singularities and Möbius strips are also ubiquitous for them.

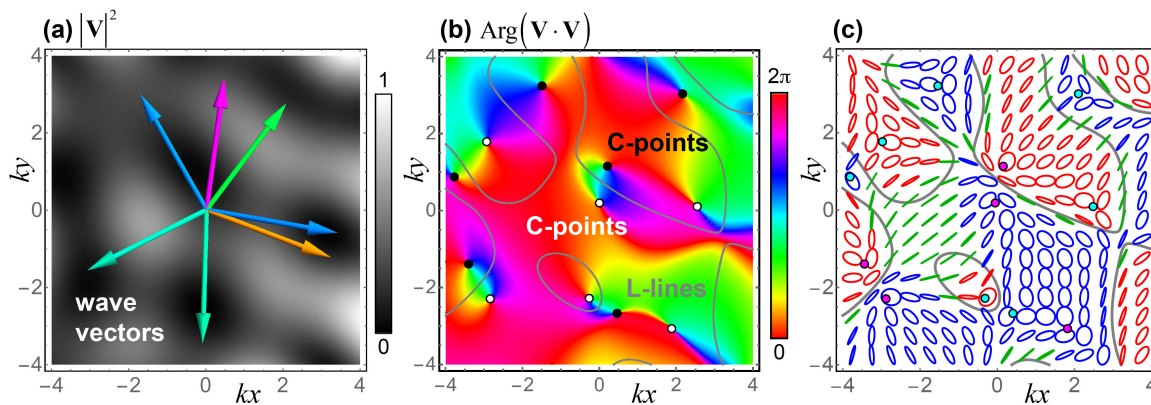


FIG. 1. Random 2D acoustic field obtained by the interference of $N = 7$ plane waves with the same frequency and amplitude but with random directions within the (x, y) plane and random phases. (a) Wavevectors of the interfering waves (with color-coded phases) and distribution of the intensity of the velocity field $|\mathbf{V}|^2$ (greyscale). (b) Color-coded distribution of the phase of the quadratic field $\mathbf{V} \cdot \mathbf{V}$. The phase singularities (vortices) of this field correspond to C-points of purely circular polarization in the field \mathbf{V} . L-lines correspond to purely linear polarizations. (c) Distribution of the normalized polarization of \mathbf{V} . Red, blue, and green colors correspond to right-handed, left-handed, and near-linear polarizations, respectively. The C-points in a 2D polarization field can be labeled by two independent topological numbers [35]: (i) $n_D = 1/2$ and $n_D = -1/2$ [black and white dots in (b), respectively] indicate half of the topological charge of the vortex in the quadratic field $\mathbf{V} \cdot \mathbf{V}$; (ii) $n_C = 1/2$ and $n_C = -1/2$ [magenta and cyan dots in (c), respectively] correspond to the number of turns of the major semiaxis of the polarization ellipse along a closed contour including the C-point.

These results can have a twofold impact. First, they provide a new platform for studying polarization singularities and topological structures. Importantly, while one cannot directly observe elliptical motion of the electric field \mathcal{E} or the vector-potential \mathcal{A} in optics, the velocity and displacement fields \mathcal{V} and \mathcal{R} are *directly observable* in acoustic and water-surface waves [11, 18, 45–47]. Second, the vector representation of sound and water-surface waves can be relevant for wave-matter interactions, such as interactions with dipole particles coupled to the vector velocity field [7, 48, 49].

The paper is organized as follows. We start by presenting the generic appearance of C-points and L-lines in random 2D acoustic fields in Section II. Section III presents polarization singularities (C-points) in 3D acoustic fields, both random and regular, as well as polarization Möbius strips which appear around C-points. Section IV demonstrates the appearance of C-points and polarization Möbius strips in structured water-surface waves. Concluding remarks are provided in Section V.

II. POLARIZATION SINGULARITIES IN A 2D ACOUSTIC FIELD

We consider monochromatic sound waves in a homogeneous fluid or gas, which are described by the equations [15]:

$$i\omega\beta P = \nabla \cdot \mathbf{V}, \quad i\omega\rho\mathbf{V} = \nabla P. \quad (1)$$

Here, ω is the frequency, ρ and β are the density and compressibility of the medium, whereas $P(\mathbf{r})$ and $\mathbf{V}(\mathbf{r})$ are the complex pressure and velocity fields. The real

time-dependent fields are $\mathcal{P}(\mathbf{r}, t) = \text{Re}[P(\mathbf{r}) \exp(-i\omega t)]$ and $\mathcal{V}(\mathbf{r}, t) = \text{Re}[\mathbf{V}(\mathbf{r}) \exp(-i\omega t)]$.

The plane-wave solution of Eqs. (1) is

$$P = P_0 \exp(i\mathbf{k} \cdot \mathbf{r}), \quad \mathbf{V} = V_0 \bar{\mathbf{k}} \exp(i\mathbf{k} \cdot \mathbf{r}), \quad (2)$$

where $\bar{\mathbf{k}} = \mathbf{k}/k$, \mathbf{k} is the wavevector, $k = \omega/c$ is the wavenumber, $c = 1/\sqrt{\rho\beta}$ is the speed of sound, and $P_0 = \sqrt{\rho/\beta} V_0$. Sound waves are longitudinal because $\mathbf{V} \parallel \mathbf{k}$, but still have a vector nature described by the velocity field \mathbf{V} [4, 6–10]. In what follows, we will focus on the polarization properties of this vector wave field: the real velocity field $\mathcal{V}(\mathbf{r}, t)$ at a given point \mathbf{r} traces a *polarization ellipse*.

We first examine a random speckle-like sound-wave field in 2D. Namely, we consider the interference of N plane waves (2), $\mathbf{V} = \sum_{j=1}^N \mathbf{V}_j$, with wavevectors \mathbf{k}_j , $j = 1, \dots, N$ randomly distributed over the circle $k_x^2 + k_y^2 = k^2$ ($k_z = 0$), and with equal amplitudes $|V_{0j}|$ but random phases $\phi_j = \text{Arg}(V_{0j})$, as shown in Fig. 1(a). Due to the longitudinal character of sound waves, $V_z = 0$, and the polarization ellipses of such field all lie in the (x, y) plane. Figure 1 shows an example of such random field including its intensity and polarization distributions.

The distributions in Fig. 1 are similar to the corresponding distributions in random paraxial electromagnetic fields, with wavevectors directed almost along the z -axis and polarization ellipses approximately lying in the (x, y) plane [19, 33, 35]. The only difference is that paraxial electromagnetic fields have a typical inhomogeneity scale of $(\theta k)^{-1}$, where $\theta \ll 1$ is the small characteristic angle between the wavevectors and the z -axis, while in the acoustic case $\theta = \pi/2$ and the typical inhomogeneity scale is k^{-1} . Polarization singularities of

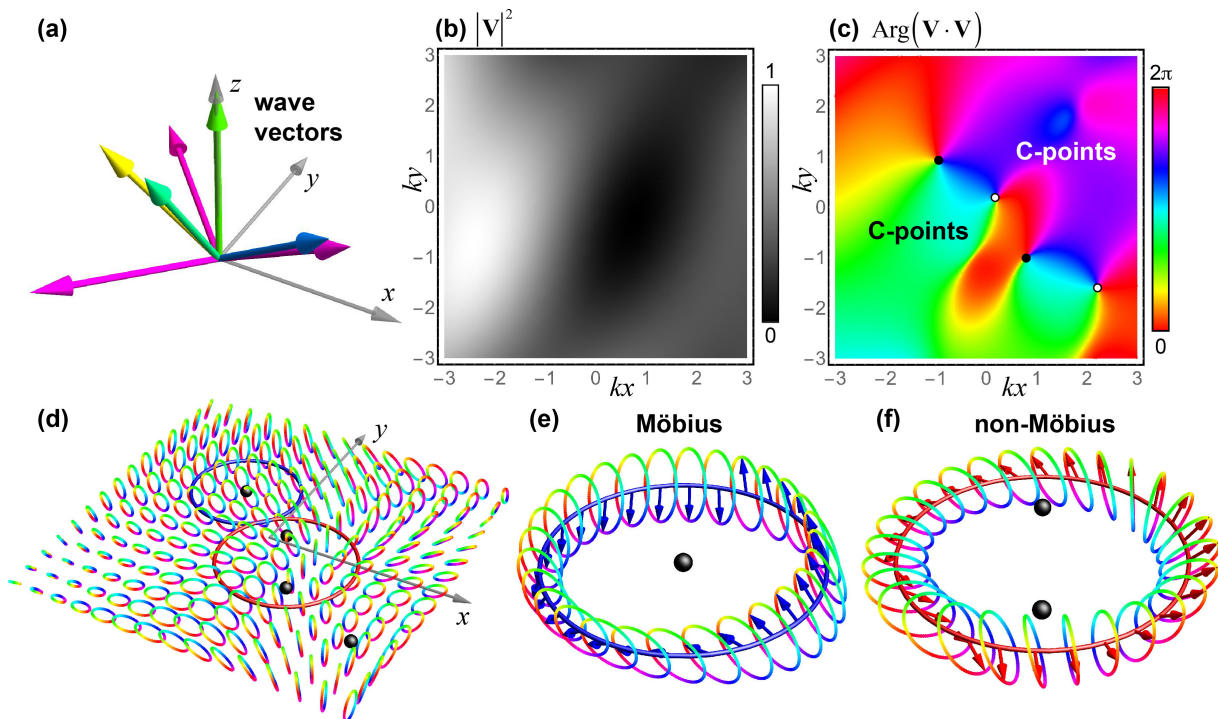


FIG. 2. Random 3D acoustic field obtained by the interference of $N = 7$ plane waves with the same frequency and amplitude but with random directions within the $k_z > 0$ semisphere and random phases. (a) Wavevectors of the interfering waves with color-coded phases. (b) Distribution of the intensity of the velocity field $|\mathbf{V}|^2$ in the $z = 0$ plane. (c) Color-coded distribution of the phase of the quadratic field $\mathbf{V} \cdot \mathbf{V}$ in the $z = 0$ plane. Phase singularities (vortices) of this field correspond to C-points of purely circular polarization in the field \mathbf{V} . (d) Distribution of the normalized polarization ellipses of \mathbf{V} in the $z = 0$ plane. (e) Continuous evolution of polarization ellipses with their major semiaxes along a contour encircling a nondegenerate C-point exhibits a Möbius-strip structure [36, 37, 39]. (f) For a contour encircling an even number of C-points (including zero), there is no polarization Möbius strip [35].

generic 2D polarization fields are the *C-points* of purely-circular polarization and *L-lines* of purely-linear polarization [19, 30, 32–35], as shown in Figs. 1(b,c).

C-points correspond to phase singularities (vortices) in the scalar field $\Psi(\mathbf{r}) = \mathbf{V}(\mathbf{r}) \cdot \mathbf{V}(\mathbf{r})$ [19, 32, 35], Fig. 1(b). Notably, these points generically coincide neither with zeros of the scalar pressure field $P(\mathbf{r})$, nor with zeros of $|\mathbf{V}(\mathbf{r})|^2$. Furthermore, each C-point in a 2D polarization field can be characterized by two half-integer topological numbers [35]. The first, n_C , corresponds to the number of turns of the major semiaxis of the polarization ellipse along a closed contour including the C-point. The second, n_D , is half the topological charge of the corresponding phase singularity in the field Ψ . In the generic (non-degenerate) case, singularities have the topological numbers $n_C = \pm 1/2$ and $n_D = \pm 1/2$ (see Fig. 1). Note that the morphological classification of 2D polarization distributions around C-points, such as ‘stars’, ‘lemons’, and ‘monstars’, is thoroughly described for optical polarized fields [19, 50] and applies here as well. Note also that higher-order singularities can appear in degenerate cases, e.g., with imposed additional symmetries, such as cylindrical beams.

III. C-POINTS AND POLARIZATION MÖBIUS STRIPS IN 3D ACOUSTIC FIELDS

A. Random fields

Akin to nonparaxial 3D electromagnetic fields, generic sound-wave fields have polarization characterized by the ellipses traced by the velocity field $\mathbf{V}(\mathbf{r}, t)$ at every point \mathbf{r} , which can be arbitrarily oriented in 3D space. To show an example of such field, we consider an interference of N plane waves with equal amplitudes $|V_{0j}|$, wavevectors \mathbf{k}_j , $j = 1, \dots, N$, with directions randomly distributed over the hemisphere $k_z > 0$ ($k_x^2 + k_y^2 + k_z^2 = k^2$), and random phases $\phi_j = \text{Arg}(V_{0j})$, see Fig. 2(a).

The distributions of the resulting intensity $|\mathbf{V}|^2$ and of the phase of the quadratic field $\mathbf{V} \cdot \mathbf{V}$ over the $z = 0$ plane are shown in Figs. 2(b,c). Similar to the 2D case, the phase singularities of the quadratic field correspond to the C-points (polarization singularities) in the polarization distribution, Fig. 2(d). However, in the 3D case, the circular polarizations in these points do not generically lie in the (x, y) plane [19, 30, 32, 35].

Furthermore, distributions of the 3D polarization ellipses in the vicinity of C-points have remarkable topo-

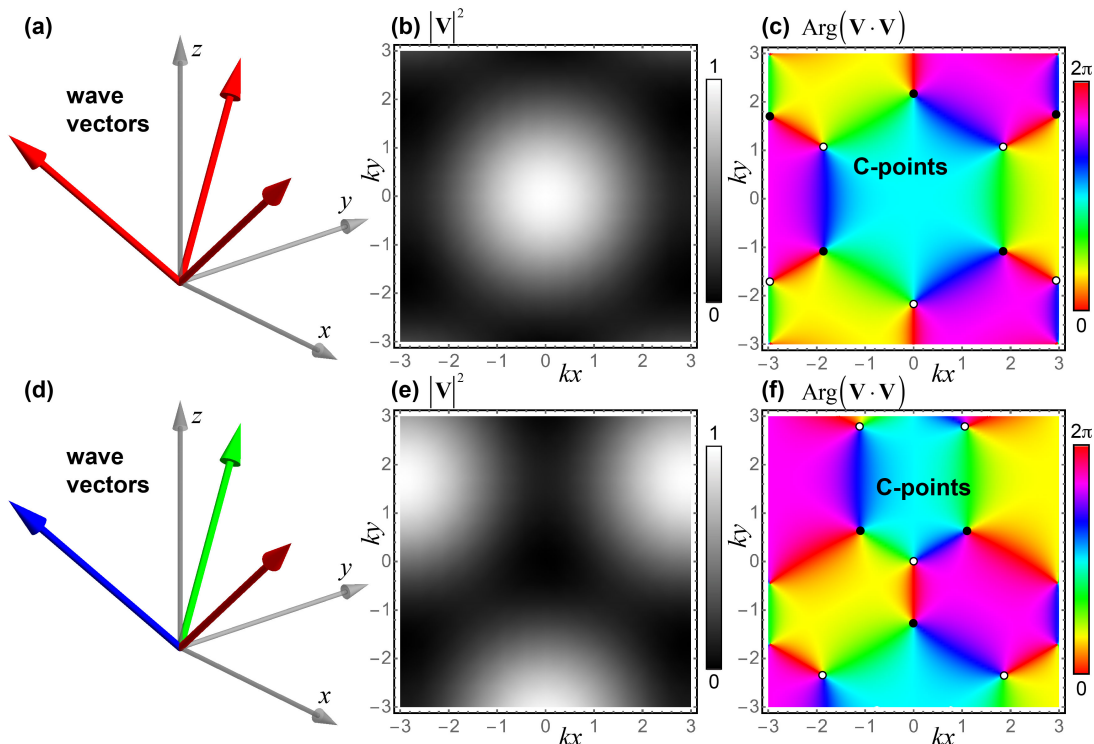


FIG. 3. The wavevectors \mathbf{k}_j , distributions of the intensity of the velocity field, $|\mathbf{V}|^2$, and of the phase of the quadratic field $\mathbf{V} \cdot \mathbf{V}$ in the $z = 0$ plane, for the three-wave superpositions (3) with $N = 3$, $\theta_0 = \pi/4$, $\ell = 0$ (a,b,c) and $\ell = 1$ (d,e,f).

logical properties. Namely, continuous evolution of the major semiaxes of the polarization ellipse along a contour encircling a non-degenerate C-point traces a 3D *Möbius-strip*-like structure [35–37, 39–44], Fig. 2(e). Notably, the number of turns of the polarization ellipse around the contour is not topologically stable: continuous deformations of the contour (without crossing C-points) can result in the change of the number of turns by an integer number [38, 51]. However, the number of turns modulo $1/2$, which distinguish the ‘Möbius’ (half-integer number of turns) and ‘non-Möbius’ (integer number of turns) cases is topologically stable. It directly corresponds to the number of C-points enclosed by the contour modulo 2 [35], see Figs. 2(d,e,f).

Recently, polarization Möbius strips attracted great attention in optics [35, 39–44]. We argue that entirely similar polarization structures naturally appear in inhomogeneous sound-wave fields. In addition to the random field shown in Fig. 2, below we consider examples of regular sound-wave fields with polarization singularities and Möbius strip.

B. Three-wave interference

We now consider examples of regular (non-random) 3D acoustic fields with polarization singularities and Möbius strips. In optics, such singularities are often generated in vector vortex beams [19, 35, 39, 40, 43, 44]. Here we

also consider a superposition of N acoustic plane waves with wavevectors evenly distributed within a cone of polar angle $\theta = \theta_0$ and with an azimuthal phase difference corresponding to a vortex of order ℓ :

$$\mathbf{V} = V_0 \sum_{j=1}^N \bar{\mathbf{k}}_j \exp[i \mathbf{k}_j \cdot \mathbf{r} + i \ell \phi_j] , \quad (3)$$

where $\mathbf{k}_j = k (\sin \theta_0 \cos \phi_j, \sin \theta_0 \sin \phi_j, \cos \theta_0)$ and $\phi_j = 2\pi(j-1)/N$. In the limit of $N \gg 1$, this superposition tends to an acoustic Bessel beam [6].

The minimal number of plane waves to generate polarization singularities is $N = 3$. Figure 3 shows the wavevectors \mathbf{k}_j , distributions of the intensity of the velocity field, $|\mathbf{V}|^2$, and of the phase of the quadratic field, $\text{Arg}(\mathbf{V} \cdot \mathbf{V})$, for the three-wave superpositions (3) with $\theta_0 = \pi/4$, $\ell = 0$ and $\ell = 1$. One can see a number of first-order C-points, i.e., phase singularities in the quadratic field $\mathbf{V} \cdot \mathbf{V}$. Accordingly, 3D polarization ellipses along a contour enclosing an odd number of C-points form polarization Möbius strips. Importantly, the spacing between the C-points in Fig. 3 is controlled by the polar angle θ_0 . When $\theta_0 \ll 1$ (paraxial regime), the C-points merge and form only *even-order* C-points with no Möbius strips around them. In particular, the four C-points at the center of Fig. 3(f) with the integer total topological charge $n_D = 3/2 - 1/2 = 1$ merge into a single second-order ($n_D = 1$) C-point in the paraxial limit. This is in sharp contrast to the electromagnetic (optical) waves,

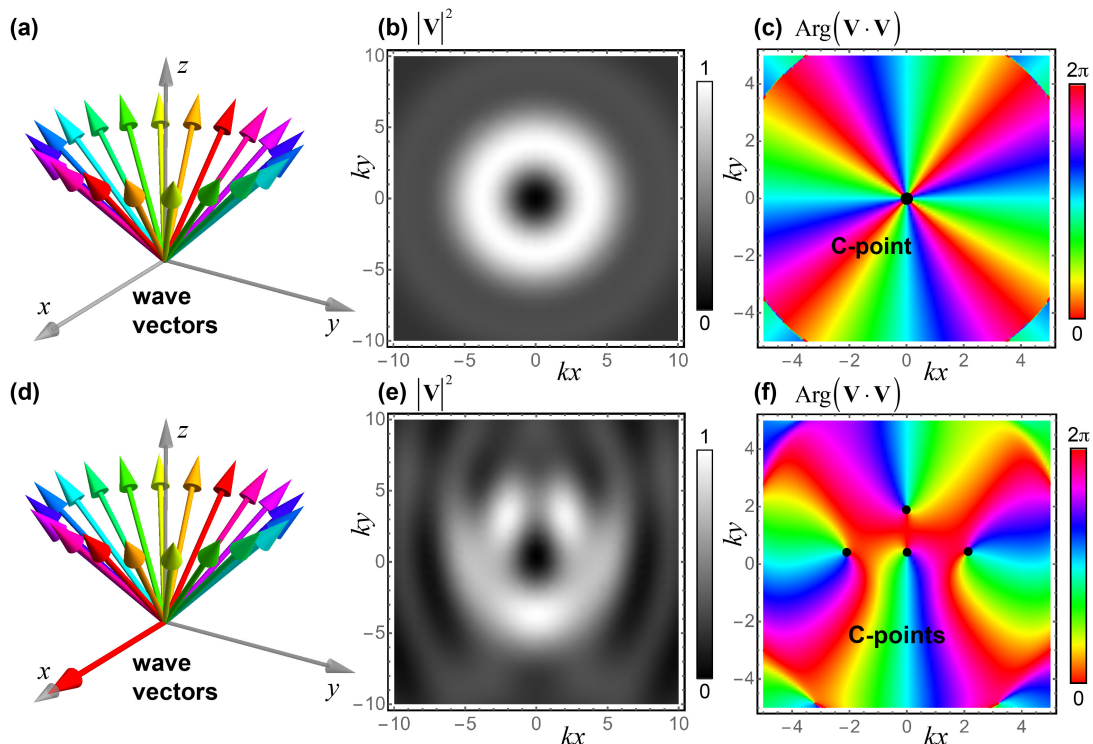


FIG. 4. The wavevectors, distributions of the intensity of the velocity field, $|\mathbf{V}|^2$, and of the phase of the quadratic field $\mathbf{V} \cdot \mathbf{V}$ in the $z = 0$ plane, for the Bessel-beam superposition (3) with $N = 20$, $\theta_0 = \pi/4$, $\ell = 2$ (a,b,c) and the same Bessel beam interfering with an additional plane wave, Eq. (4), with $V'/V_0 = 2$ (d,e,f). One can see the splitting of the even-order C-point (integer $n_D = \ell$) (c) into $2|n_D|$ first-order C-points (f) when breaking the cylindrical symmetry of the vortex beam.

where isolated first-order C-points can appear even in the paraxial case.

C. Perturbed vortex beams

Consider now the large- N limit of the superposition (3), which generates acoustic vortex (Bessel) beams. Due to the cylindrical symmetry, such beams can have an isolated C-point at the center. However, in contrast to optical vectorial vortex beams, the C-point at the center of an acoustic vortex beam always has an even order (integer $n_D = \ell$) [6] (see Fig. 4). This does not allow one to generate an acoustic polarization Möbius strip in a symmetric vortex configuration as in optics [35, 39, 40, 43, 44]. However, breaking the cylindrical symmetry of the beam results in splitting of the even-order C-point at the center into a number of the first-order C-points ($n_D = \pm 1/2$), each of which carries polarization Möbius strip structures around it. For example, one can break the symmetry by interfering the vortex beam with a horizontally-propagating plane wave:

$$\mathbf{V} = \mathbf{V}_{\text{vortex}} + V' \bar{\mathbf{k}}' \exp(i \mathbf{k}' \cdot \mathbf{r}), \quad (4)$$

where $\mathbf{V}_{\text{vortex}}$ is the vortex-beam field, such as Eq. (3) with $N \gg 1$, whereas $\mathbf{k}' = k(1, 0, 0)$. Figure 4 shows the splitting of the even-order C-point at the center of an

acoustic vortex beam into first-order C-points when interfering the beam with a horizontally-propagating plane wave.

The above examples show that the typical spacing between the C-points in structured sound waves is k^{-1} , and this spacing can decrease in the paraxial regime and in the presence of additional symmetries. This also determines the typical subwavelength size of the acoustic polarization Möbius strips.

IV. POLARIZATION SINGULARITIES AND MÖBIUS STRIPS IN WATER-SURFACE WAVES

One of the key differences between electromagnetic and acoustic fields is that the electric and magnetic fields are vectors in abstract spaces of the field components (there is no ‘ether’ and nothing moves in a free-space electromagnetic wave), while the velocity field corresponds to the motion of the medium’s particles (atoms or molecules) in real space. Moreover, instead of the velocity field, one can consider the *displacement* field $\mathcal{R}(\mathbf{r}, t)$: $\mathbf{V} = \partial_t \mathcal{R}$, or, for a monochromatic field in the complex representation, $\mathbf{V} = -i\omega \mathbf{R}$. The displacement field can be regarded as a ‘vector-potential’ for the velocity field [10]. It has the same polarization, but the polarization ellipses traced by \mathcal{R} correspond to *real-space trajectories*

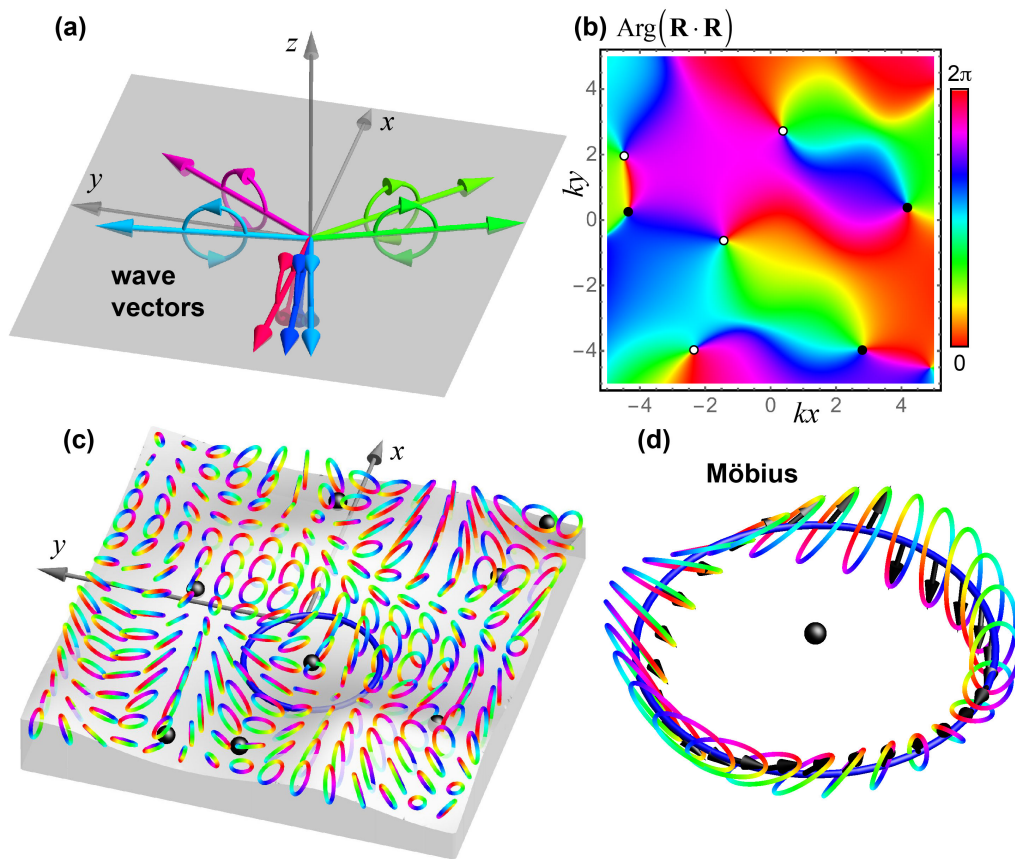


FIG. 5. Random 3D water-surface wave field obtained by the interference of $N = 7$ plane waves with the same frequency and amplitude but with random directions in the (x, y) plane and random phases. (a) Wavevectors of the interfering waves with color-coded phases and their circular polarizations. (b) Color-coded distribution of the phase of the quadratic field $\mathbf{R} \cdot \mathbf{R}$ in the water-surface $z = 0$ plane. Phase singularities (vortices) of this field correspond to C-points of purely circular polarization in the field \mathbf{R} . (c) Distribution of the normalized polarization ellipses of the \mathbf{R} field in the $z = 0$ plane. These ellipses are trajectories of water-surface particles (Multimedia view). The instantaneous water surface at $t = 0$ is shown in gray. (d) Akin to Fig. 2, the continuous evolution of polarization ellipses with their major semiaxes along a contour encircling a C-point exhibits a polarization Möbius strip (Multimedia view).

of the medium particles.

This opens an avenue to the *direct observation* of polarization ellipses and more complicated structures [12]. In sound waves, typical displacement amplitudes are small and their direct observations are challenging [45, 46]. However, similar medium displacements can be easily observed in another type of classical waves, namely, *water-surface* (e.g., *gravity or capillary*) waves [15], with typical displacement scales ranging from millimeters to meters. Recently, there were several studies on polarization properties of structured water waves [11, 12, 47], and here we show that these waves naturally reveal generic polarization singularities.

For the sake of simplicity, we consider deep-water gravity waves on the unperturbed water surface $z = 0$ [15]. The equations of motion for the complex displacement field $\mathbf{R} = (X, Y, Z)$ of the water-surface particles in a monochromatic wave field can be written in a form sim-

ilar to the acoustic equations (1) [11, 12]:

$$\omega^2 Z = -g \nabla_{\perp} \cdot \mathbf{R}_{\perp}, \quad \omega^2 \mathbf{R}_{\perp} = g \nabla_{\perp} Z. \quad (5)$$

Here g is the gravitational acceleration, $\mathbf{R}_{\perp} = (X, Y)$, and $\nabla_{\perp} = (\partial_x, \partial_y)$. Making the plane-wave ansatz $\nabla_{\perp} \rightarrow i \mathbf{k}$, $\mathbf{k} = (k_x, k_y)$, in Eqs. (5), we obtain the dispersion relation $\omega^2 = gk$.

The plane-wave solution of Eqs. (5) is:

$$Z = Z_0 \exp(i \mathbf{k} \cdot \mathbf{r}), \quad \mathbf{R}_{\perp} = i Z_0 \bar{\mathbf{k}} \exp(i \mathbf{k} \cdot \mathbf{r}). \quad (6)$$

These relations show that deep-water gravity waves have equal longitudinal (\mathbf{k} -directed) and transverse (z -directed) displacement components phase-shifted by $\pi/2$ with respect to each other. In other words, such plane waves are *circularly polarized* in the meridional (propagation) plane including the wavevector and the normal to the unperturbed water surface [18]. Such (generically, elliptical) meridional polarization is a common feature of surface and evanescent waves in different physical contexts [4, 5, 16, 17]. Therefore, interfering plane water

waves with wavevectors lying in the (x, y) plane results in generic 3D polarization structures with all three components of the displacement field \mathbf{R} .

To show that such polarization distributions generically possess polarization singularities, we consider the interference of N plane waves (6): $\mathbf{R} = \sum_{j=1}^N \mathbf{R}_j \equiv \sum_{j=1}^N \mathbf{R}_{0j} \exp(i\mathbf{k}_j \cdot \mathbf{r}_\perp)$, with $\mathbf{R}_{0j} = Z_{0j}(i\bar{k}_{jx}, i\bar{k}_{jy}, 1)$, wavevectors \mathbf{k}_j randomly distributed over the circle $k_x^2 + k_y^2 = k^2$, and equal amplitudes $|Z_{0j}|$ but random phases $\phi_j = \text{Arg}(Z_{0j})$, as shown in Fig. 5(a) (cf. Fig. 1). Figure 5(b) shows the phase distribution of the quadratic field $\Psi = \mathbf{R} \cdot \mathbf{R}$; it clearly exhibits phase singularities corresponding to C-points of the vector field \mathbf{R} . The distribution of the polarization ellipses, i.e., trajectories of the water-surface particles, over the $z = 0$ plane is shown in Fig. 5(c) (Multimedia view). Tracing the orientation of the polarization ellipses along a contour encircling a C-point reveals the generic Möbius-strip structure, Fig. 5(d) (Multimedia view). We also provide animated versions of Figs. 5(c,d), where one can see motion of the water surface and separate water particles. In particular, the animated version of Fig. 5(d) shows the temporal evolution of the displacement vectors $\mathcal{R}(\mathbf{r}, t)$ along the contour, which can form ‘twisted ribbon carousels’ [52].

Thus, by tracing 3D trajectories of water particles in a random (yet monochromatic) water-surface wavefield one can directly observe generic polarization singularities of 3D vector wavefields.

V. CONCLUDING REMARKS

This work was motivated by recent strong interest in (i) polarization Möbius strips in 3D polarized optical fields [35–44] and (ii) vectorial spin properties of acoustic and water-surface waves [4–12]. We have shown that these research directions can be naturally coupled, and that polarization singularities, such as C-points and polarization Möbius strips, are ubiquitous for inhomogeneous (yet monochromatic) acoustic and water-surface waves. The vector velocity or displacement of the medium particles provide complex-valued elliptical polarization fields varying across the space. We have considered various examples of random and regular interference fields consisting of multiple (three or more) plane waves, which exhibit polarization singularities and Möbius strips.

In contrast to well-studied electromagnetic polarizations associated with the motion of abstract field vectors, acoustic and water-wave polarizations correspond to real-space trajectories of the medium particles. In particular, these are readily directly observable for water-surface waves [11, 47]. Also, while optical vectorial-vortex beams can bear an isolated first-order C-point and a Möbius strip around it [35, 39, 40, 43, 44], acoustic C-points typically appear in clusters with subwavelength distance be-

tween the points.

Analyzing wave-field singularities is useful because of their topological robustness; they provide a ‘skeleton’ of an inhomogeneous field [53]. This robustness is highly important because real-life waves in fluids always have inherent perturbations, such as viscosity and nonlinearity, with respect to the idealized non-dissipative linear picture. So far, only *phase* singularities of the *scalar* pressure field P were considered in sound-wave fields. The vector velocity field $\mathbf{V} \propto \nabla P$ and its polarization singularities provide an alternative representation and can be more relevant, e.g., in problems involving dipole wave-matter coupling. Note that the vectorial representation of a gradient of a scalar wavefield was previously considered in Ref. [54].

For water-surface waves, the scalar representation is based on the vertical displacement field Z . Tidal ocean waves were also studied in terms of the 2D polarization field of the horizontal current [27–29, 55, 56] associated with the velocity components (V_x, V_y) . We argue that these scalar and 2D vector fields can be regarded as components of a single 3D vector displacement \mathbf{R} or velocity \mathbf{V} field. Moreover, we have considered gravity deep-water waves, which are much more feasible for experimental laboratory studies than tidal waves [11, 47].

Notably, our arguments are not restricted to purely sound and water-surface waves. They can be equally applied to any fluid/gas or fluid/fluid surface waves as well as internal gravity waves in stratified fluid or gas media. We hope that our work will stimulate further studies and possibly applications of 3D polarization textures and topological vectorial properties of various waves in acoustics and fluid mechanics.

ACKNOWLEDGMENTS

M.A.A. was supported by the Excellence Initiative of Aix Marseille University—A*MIDEX, a French ‘Investissements d’Avenir’ programme. F.N. was supported by Nippon Telegraph and Telephone Corporation (NTT) Research; the Japan Science and Technology Agency (JST) via the Quantum Leap Flagship Program (Q-LEAP), the Moonshot R&D Grant No. JP- MJMS2061, and the Centers of Research Excellence in Science and Technology (CREST) Grant No. JPMJCR1676; the Japan Society for the Promotion of Science (JSPS) via the Grants-in-Aid for Scientific Research (KAKENHI) Grant No. JP20H00134, and the JSPS-RFBR Grant No. JPJSBP120194828; the Army Research Office (ARO) (Grant No. W911NF-18-1-0358); the Asian Office of Aerospace Research and Development (AOARD) (Grant No. FA2386-20-1-4069); and the Foundation Questions Institute Fund (FQXi) (Grant No. FQXi-IAF19-06).

- [1] R. M. A. Azzam and N. M. Bashara, *Ellipsometry and polarized light* (North-Holland, 1977).
- [2] D. L. Andrews and M. Babiker, eds., *The Angular Momentum of Light* (Cambridge University Press, 2012).
- [3] V. B. Berestetskii, E. M. Lifshitz, and L. P. Pitaevskii, *Quantum Electrodynamics* (Pergamon Press, Oxford, 1982).
- [4] C. Shi, R. Zhao, Y. Long, S. Yang, Y. Wang, H. Chen, J. Ren, and X. Zhang, “Observation of acoustic spin,” *Natl. Sci. Rev.* **6**, 707 (2019).
- [5] K. Y. Bliokh and F. Nori, “Transverse spin and surface waves in acoustic metamaterials,” *Phys. Rev. B* **99**, 020301(R) (2019).
- [6] K. Y. Bliokh and F. Nori, “Spin and orbital angular momenta of acoustic beams,” *Phys. Rev. B* **99**, 174310 (2019).
- [7] I. D. Toftul, K. Y. Bliokh, M. I. Petrov, and F. Nori, “Acoustic radiation force and torque on small particles as measures of the canonical momentum and spin densities,” *Phys. Rev. Lett.* **123**, 183901 (2019).
- [8] I. Rondón and D. Leykam, “Acoustic vortex beams in synthetic magnetic fields,” *J. Phys.: Cond. Mat.* **32**, 104001 (2019).
- [9] Y. Long, D. Zhang, C. Yang, J. Ge, H. Chen, and J. Ren, “Realization of acoustic spin transport in metasurface waveguides,” *Nat. Commun.* **11**, 4716 (2020).
- [10] L. Burns, K. Y. Bliokh, F. Nori, and J. Dressel, “Acoustic versus electromagnetic field theory: scalar, vector, spinor representations and the emergence of acoustic spin,” *New J. Phys.* **22**, 053050 (2020).
- [11] K. Y. Bliokh, H. Punzmann, H. Xia, F. Nori, and M. Shats, “Relativistic field-theory spin and momentum in water waves,” arXiv:2009.03245 (2020).
- [12] D. Sugic, M. R. Dennis, F. Nori, and K. Y. Bliokh, “Knotted polarizations and spin in 3D polychromatic waves,” *Phys. Rev. Research* **2**, 042045(R) (2020).
- [13] W. L. Jones, “Asymmetric wave-stress tensors and wave spin,” *J. Fluid Mech.* **58**, 737–747 (1973).
- [14] M. S. Longuet-Higgins, “Spin and angular momentum in gravity waves,” *J. Fluid Mech.* **97**, 1–25 (1980).
- [15] L. D. Landau and E. M. Lifshitz, *Fluid Mechanics* (Butterworth-Heinemann, Oxford, 1987).
- [16] K. Y. Bliokh and F. Nori, “Transverse and longitudinal angular momenta of light,” *Phys. Rep.* **592**, 1–38 (2015).
- [17] A. Aiello, P. Banzer, M. Neugebauer, and G. Leuchs, “From transverse angular momentum to photonic wheels,” *Nat. Photon.* **9**, 789–795 (2015).
- [18] www.saddleback.edu/faculty/jrepka/notes/waves.html.
- [19] M. R. Dennis, K. O’Holleran, and M. J. Padgett, “Singular optics: Optical vortices and polarization singularities,” *Prog. Opt.* **53**, 293–363 (2009).
- [20] J. Eggers, “Role of singularities in hydrodynamics,” *Phys. Rev. Fluids* **3**, 110503 (2018).
- [21] H. K. Moffatt, “Singularities in fluid mechanics,” *Phys. Rev. Fluids* **4**, 110502 (2019).
- [22] D. Kleckner and W. T. M. Irvine, “Creation and dynamics of knotted vortices,” *Nat. Phys.* **9**, 253–258 (2013).
- [23] H. Zhang, W. Zhang, Y. Liao, X. Zhou, J. Li, G. Hu, and X. Zhang, “Creation of acoustic vortex knots,” *Nat. Commun.* **11**, 3956 (2020).
- [24] H. Chen and J.-C. Meiners, “Topologic mixing on a microfluidic chip,” *Appl. Phys. Lett.* **84**, 2193–2195 (2004).
- [25] R. E. Goldstein, H. K. Moffatt, A. I. Pesci, and R. L. Ricca, “Soap-film Möbius strip changes topology with a twist singularity,” *Proc. Natl. Acad. Sci. USA* **107**, 21979–21984 (2010).
- [26] W. Whewell, “On the results of an extensive series of tide observations,” *Phil. Trans. Roy. Soc. Lond.* , 289–307 (1836).
- [27] W. Hansen, *Gezeiten und Gezeitenströme der halbtägigen Hauptmond tide M2 in der Nordsee* (Hamburg: Deutsche Hydrographisches Institut, 1952).
- [28] M. V. Berry, “Geometry of phase and polarization singularities, illustrated by edge diffraction and the tides,” *Proc. SPIE* **4403**, 1 (2001).
- [29] J. F. Nye, J. V. Hajnal, and J. H. Hannay, “Phase saddles and dislocations in two-dimensional waves such as the tides,” *Proc. Roy. Soc. Lond. A* **417**, 7–20 (1988).
- [30] J. F. Nye and J. V. Hajnal, “The wave structure of monochromatic electromagnetic radiation,” *Proc. Roy. Soc. Lond. A* **409**, 21–36 (1987).
- [31] M. S. Soskin and M. V. Vasnetsov, “Singular optics,” *Prog. Opt.* **42**, 219–276 (2001).
- [32] M. V. Berry and M. R. Dennis, “Polarization singularities in isotropic random vector waves,” *Proc. R. Soc. Lond. A* **457**, 141 (2001).
- [33] J. F. Nye, “Lines of circular polarization in electromagnetic wave fields,” *Proc. Roy. Soc. Lond. A* **389**, 279–290 (1983).
- [34] J. V. Hajnal, “Singularities in the transverse fields of electromagnetic waves. II. Observations on the electric field,” *Proc. R. Soc. Lond. A* **414**, 447–468 (1987).
- [35] K. Y. Bliokh, M. A. Alonso, and M. R. Dennis, “Geometric phases in 2D and 3D polarized fields: geometrical, dynamical, and topological aspects,” *Rep. Prog. Phys.* **82**, 122401 (2019).
- [36] I. Freund, “Optical Möbius strips in three-dimensional ellipse fields: I. Lines of circular polarization,” *Opt. Commun.* **283**, 1–15 (2010).
- [37] I. Freund, “Multitwist optical Möbius strips,” *Opt. Lett.* **35**, 148–150 (2010).
- [38] M. R. Dennis, “Fermionic out-of-plane structure of polarization singularities,” *Opt. Lett.* **36**, 3765–3767 (2011).
- [39] T. Bauer, P. Banzer, E. Karimi, S. Orlov, A. Rubano, L. Marrucci, E. Santamato, R. W. Boyd, and G. Leuchs, “Observation of optical polarization Möbius strips,” *Science* **347**, 964–966 (2015).
- [40] E. J. Galvez, I. Dutta, K. Beach, J. J. Zeosky, J. A. Jones, and B. Khajavi, “Multitwist Möbius strips and twisted ribbons in the polarization of paraxial light beams,” *Sci. Rep.* **7**, 13653 (2017).
- [41] A. Garcia-Etxarri, “Optical polarization Möbius strips on all-Dielectric optical scatterers,” *ACS Photon.* **4**, 1159–1164 (2017).
- [42] J. Kreissmann and M. Hentschel, “The optical Möbius strip cavity: Tailoring geometric phases and far fields,” *EPL* **121**, 24001 (2018).
- [43] T. Bauer, P. Banzer, F. Bouchard, S. Orlov, L. Marrucci, E. Santamato and R. W. Boyd, E. Karimi, and G. Leuchs, “Multi-twist polarization ribbon topologies in highly-confined optical fields,” *New J. Phys.* **21**, 053020 (2019).

- [44] K. Tekce, E. Otte, and C. Denz, “Optical singularities and Möbius strip arrays in tailored non-paraxial light fields,” *Opt. Express* **27**, 29685–29696 (2019).
- [45] K. J. Taylor, “Absolute measurement of acoustic particle velocity,” *J. Acoust. Soc. Am.* **59**, 691–694 (1976).
- [46] T. B. Gabrielson, D. L. Gardner, and S. L. Garrett, “A simple neutrally buoyant sensor for direct measurement of particle velocity and intensity in water,” *J. Acoust. Soc. Am.* **97**, 2227–2237 (1995).
- [47] N. Francois, H. Xia, H. Punzmann, P. W. Fontana, and M. Shats, “Wave-based liquid-interface metamaterials,” *Nat. Commun.* **8**, 14325 (2017).
- [48] L. Wei and F. J. Rodriguez-Fortuno, “Far-field and near-field directionality in acoustic scattering,” *New J. Phys.* **22**, 083016 (2020).
- [49] Y. Long, H. Ge, D. Zhang, X. Xu, J. Ren, M.-H. Lu, M. Bao, H. Chen, and Y.-F. Chen, “Symmetry selective directionality in near-field acoustics,” *Natl. Sci. Rev.* **7**, 1024–135 (2020).
- [50] M. R. Dennis, “Polarization singularities in paraxial vector fields: morphology and statistics,” *Opt. Commun.* **213**, 201–221 (2002).
- [51] I. Freund, “Polarization Möbius strips on elliptical paths in three-dimensional optical fields,” *Opt. Lett.* **45**, 3333–3336 (2020).
- [52] I. Freund, “Twisted ribbon carousels in random, three-dimensional optical fields,” *Opt. Lett.* **45**, 5905–5908 (2020).
- [53] J. Nye, *Natural focusing and fine structure of light* (IOP Publishing, Bristol, 1999).
- [54] M. R. Dennis, “Local phase structure of wave dislocation lines: twist and twirl,” *J. Opt. A: Pure Appl. Opt.* **6**, S202–S208 (2004).
- [55] R. D. Ray, “Inversion of oceanic tidal currents from measured elevations,” *J. Mar. Syst.* **28**, 1–18 (2001).
- [56] R. D. Ray and G. D. Egbert, “The Global S1 Tide,” *J. Phys. Oceanogr.* **34**, 1922–1935 (2004).